

13A.4 Using Enstrophy Transport as a Diagnostic to Identify Flow Regime Transformation

Andrew D. Jensen^{*1}, Anthony R. Lupo¹, and Igor I. Mokhov²

¹Department of Soil, Environmental, and Atmospheric Science, University of Missouri-Columbia

²A.M. Obukhov Institute of Atmospheric Physics, Russian Academy of Sciences

1 Introduction

The phenomenon of blocking can make local and regional forecasting less reliable [1]. However, previous results have shown that with the use of certain stability indices both the onset and decay of blocking may be relatively easier to diagnose [1, 7, 8]. The aforementioned results showed that in an approximately barotropic flow the sum of the positive local Lyapunov exponents is approximated well by integrating enstrophy (squared vorticity) over a finite bounded region. This quantity has been termed area integrated enstrophy (IRE) and it can be used to determine the stability or predictability within a flow regime [7]. More specifically, low values of IRE imply a more predictable or stable state, while high values of IRE imply a more unstable state in the flow. IRE has been used successfully to identify the onset and decay of blocking states in the atmosphere. It was shown in [7] that the IRE reaches a relative maximum value at block onset and decay, while it decreases to a relative minimum during the block as the flow stabilizes.

The IRE may have utility beyond the detection of blocking onset and decay. It may also be an effective diagnostic to identify flow regime change generally. The weakness in this technique is locating a certain threshold value at which the flow can be identified as having undergone regime transformation. In this work we have identified the advection of enstrophy as a useful diagnostic in identifying blocking onset and decay, and potentially even more general regime change. To that end, several blocking events were tested and the enstrophy advection was found to be a useful diagnos-

tic. In addition, the criterion of Weiss [12], which is similar to fluid trapping [4] and which we use synonymously, can be employed to locate strain dominated regions of the flow and in conjunction with the enstrophy advection it is conjectured to be useful in identifying blocking regions. A new equation based on fluid trapping is then derived that shows the physical processes behind the way in which enstrophy advection works as a diagnostic. The second part of the paper is concerned with applications of the diagnostics to four Northern Hemisphere blocking occurrences.

The purpose of this work is to demonstrate that by the use of IRE and enstrophy advection blocking events can be more successfully identified, which may lead to more accurate forecasting of blocking. The simplicity of enstrophy advection as a stability index may make it particularly useful as a diagnostic in forecasting situations.

2 Local Lyapunov Exponents

The stability characteristics mentioned above, IRE and enstrophy advection, were derived from a careful consideration of local Lyapunov exponents for the barotropic vorticity equation. Therefore, a brief description of local Lyapunov exponents is not out of place. These are defined by $\lambda_i(\zeta_0, T) = \frac{1}{2n} \log \nu_i$ for an initial vorticity field ζ_0 and time $T = n\Delta t$. The ν_i are the eigenvalues of M^*M , where $M = \prod_{k=-n}^{k=n} A(k\Delta t)$ and $A(t)$ is the linearization operator of the barotropic vorticity equation at $\zeta(t)$. The local Lyapunov exponents thus provide a measure of divergence of nearby trajectories for small time.

In order to show that the IRE is approximated by the sum of the positive local Lyapunov exponents the barotropic vorticity equation for an incompressible, inviscid fluid is considered. We now sketch the argument given in [5]. For a given

^{*}Corresponding author address: Andrew Jensen, Department of Soil, Environmental, and Atmospheric Sciences, 302 Anheuser Busch Natural Resources Building, University of Missouri, Columbia, MO, 65211; jensenad@missouri.edu

streamfunction Ψ , where $\nabla^2\Psi = \zeta$, the barotropic vorticity equation can be written in the form,

$$\frac{\partial \nabla^2\Psi}{\partial t} + J(\Psi, \nabla^2\Psi) = 0. \quad (1)$$

To model blocked flow, a streamfunction of the form

$$\Psi = \bar{\psi}(y) + \psi'(x, y) \quad (2)$$

can be considered, where

$$\psi'(x, y) = \psi(y)e^{ikx}, \quad (3)$$

i.e., Ψ describes a zonal flow with superimposed stationary waves [2].

Now a Crank-Nicholson scheme can be applied to the linearized barotropic vorticity equation to obtain the result that the enstrophy integrated over a finite and bounded region can be approximated with reasonable accuracy by the sum of the positive local Lyapunov exponents. It was found in [5] that the eigenvalues of the the operator $A + A^*$, where A is the linearization operator, are a good approximation of the local Lyapunov exponents for small values of time.

3 IRE

Recent work [1, 5, 7, 8] has shown the value of the IRE as a diagnostic for block onset and block decay. As shown in [7], the IRE was found to increase sharply at block onset, and then decrease to a local minimum. The IRE was seen to increase again at block decay. This dynamical behavior was shown to occur for several case studies [1, 7, 8]. In particular, in [7] it was shown to occur for three winter season blocking events in the Southern Hemisphere. Moreover, in [1] the IRE was used to examine a three year period of blocking occurrences across the entire Northern Hemisphere with similar results. In [8] the block that occurred over the European part of Russia that brought devastating high temperatures was considered and similar results were obtained. It is believed that the dynamical behavior of blocks shown by the IRE holds generally.

4 Enstrophy Advection

As was shown in [5] and as sketched in section (2) above, to a good approximation we may take

$$\sum_{\lambda_i > 0} \lambda_i \approx \int \zeta^2, \quad (4)$$

where the integral is over a fixed, finite, bounded region. Note that the $\lambda_i > 0$ change with time, and thus we may consider the change of their sum, $\sum_{\lambda_i > 0} \lambda_i$, with time as follows. We use the transport theorem and differentiate (4) under the integral:

$$\begin{aligned} \frac{d(\sum_{\lambda_i > 0} \lambda_i)}{dt} &\approx \frac{d}{dt} \int \zeta^2 \\ &= \int \frac{\partial \zeta^2}{\partial t} = \int 2\zeta \frac{\partial \zeta}{\partial t} \\ &= - \int 2\zeta V \cdot \nabla \zeta = - \int V \cdot \nabla \zeta^2, \end{aligned} \quad (5)$$

where we have assumed an incompressible frictionless barotropic flow. Therefore, the change in the stability characteristic over time can be approximated by the integral $-\int V \cdot \nabla \zeta^2$. Moreover, since the quantity $-V \cdot \nabla \zeta^2$ determines the sign of the integral we may consider the enstrophy advection, $-V \cdot \nabla \zeta^2$, as an indicator of stability. The dynamical stability can be determined in the following way. If $-V \cdot \nabla \zeta^2 < 0$, the flow is becoming more stable. On the other hand, if $-V \cdot \nabla \zeta^2 > 0$, the flow is becoming more unstable. Regions in which $-V \cdot \nabla \zeta^2$ changes from negative to positive are where a local maximum in instability is expected.

Another way of obtaining a similar result is by considering Lyapunov functions. A Lyapunov function is a positive definite function which can be used to show the Lyapunov stability or instability of a flow by either the positivity or negativity of the derivative, respectively. In fact, $V(\zeta) = \int \zeta^2$ can be taken as a Lyapunov function. Then, by taking the material derivative of V , similar results as above are achieved.

More concretely, a function $V(x)$ is called positive definite if it is positive everywhere in some domain, but with $V(0) = 0$. Consider the differential equation $\frac{dx}{dt} = f(x)$, defined for all x in some domain. If $f(0) = 0$ and there exists a function $V(x)$ defined in a neighborhood of $x = 0$ such that $\frac{d}{dt}V(x)$ is positive in a neighborhood of $x = 0$, then the equilibrium solution is unstable in the sense of Lyapunov. That is, initially close trajectories diverge. This theorem can be applied to the system of differential equations $\frac{d\zeta^2}{dt} = 0$ to obtain a result similar to that in equation (5).

5 Fluid Trapping

Another potentially useful diagnostic for determining stability in a barotropic flow is the Okubo-Weiss criterion; see [12]. In [12], Weiss considered a two-dimensional, inviscid, incompressible fluid.

Taking the symmetric part of the stress tensor S , and in order to simplify calculations, the following quantities θ, ψ, μ were defined as $\theta = \frac{\partial u}{\partial x} - \frac{\partial v}{\partial y}$, $\psi = \frac{\partial v}{\partial x} + \frac{\partial u}{\partial y}$, and $\mu = \theta + i\psi$. It was found that

$$\text{tr}S^2 = \frac{1}{2} (\mu\bar{\mu} - \zeta^2) \quad (6)$$

where ζ is the relative vorticity. It can also be shown that incompressibility implies

$$\text{div}(V \cdot \nabla V) = \frac{1}{2} (\mu\bar{\mu} - \zeta^2). \quad (7)$$

Equation (6) or (7) can be used to locate regions in the fluid that are strain dominated and regions that are vorticity dominated by means of the sign of (7), i.e., either positive or negative. While considering the enstrophy cascade in two-dimensional turbulence, it was shown in [3] that enstrophy advection should be preferentially positive in regions that are strain dominated, that is, where $(\mu\bar{\mu} - \zeta^2) > 0$. Thus, the Okubo-Weiss criterion can likely be successfully used with enstrophy advection to determine regions of stability or instability in the flow.

If it holds true that regions of strain are turbulent in a two-dimensional sense, then the hypothesis of frictionless flow can be dropped and we can start with the barotropic vorticity equation in the form [10]

$$\frac{d}{dt}\zeta = \frac{1}{R}\nabla^2\zeta, \quad (8)$$

where R is the Reynolds number. Then it can be shown that

$$\frac{d}{dt}\int\zeta^2 = -\frac{2}{R}\int(\nabla\zeta)^2, \quad (9)$$

for small Reynolds numbers. Thus, the stability implied by (9) may hold at times between block onset and decay. For large Reynolds numbers on the other hand, or as $R \rightarrow \infty$, our original calculation goes through without change. This may apply at block onset and decay.

Weiss's original assumption of a slowly varying μ may not hold for large times. However, for blocking, which can be thought of as a synoptic scale phenomenon with time measured in days, we believe the time scale to be sufficiently small for the Okubo-Weiss criterion to be useful.

6 Advection Equation

Now, using fluid trapping, an equation is derived which elucidates the physical processes by which

enstrophy is advected in an incompressible, frictionless barotropic flow. First, the horizontal equations of motion are considered, in the form

$$\frac{\partial u}{\partial t} + u\frac{\partial u}{\partial x} + v\frac{\partial u}{\partial y} = -\frac{\partial\phi}{\partial x} + fv + F_x$$

and

$$\frac{\partial v}{\partial t} + u\frac{\partial v}{\partial x} + v\frac{\partial v}{\partial y} = -\frac{\partial\phi}{\partial y} - fu + F_y$$

where the F terms represent friction/viscosity. Now, the divergence of the equations can be taken:

$$\begin{aligned} \frac{\partial}{\partial x} \left(\frac{\partial u}{\partial t} + u\frac{\partial u}{\partial x} + v\frac{\partial u}{\partial y} = -\frac{\partial\phi}{\partial x} + fv + F_x \right) \\ + \\ \frac{\partial}{\partial y} \left(\frac{\partial v}{\partial t} + u\frac{\partial v}{\partial x} + v\frac{\partial v}{\partial y} = -\frac{\partial\phi}{\partial y} - fu + F_y \right) \end{aligned}$$

Note that since we have assumed incompressibility the continuity equation is simply

$$\frac{\partial u}{\partial x} + \frac{\partial v}{\partial y} = 0, \quad (10)$$

or $\frac{\partial u}{\partial x} = -\frac{\partial v}{\partial y}$. This can be used to simplify the divergence above to get

$$2 \left(\frac{\partial v}{\partial x} \frac{\partial u}{\partial y} - \frac{\partial u}{\partial x} \frac{\partial v}{\partial y} \right) = -\nabla^2\phi + f\zeta \quad (11)$$

where ζ is relative vorticity.

Recall that the Okubo-Weiss criterion is $\frac{1}{2}(E^2 - \zeta^2)$, where $\mu\bar{\mu} = E^2$ and E is the total deformation. The expression $\frac{1}{2}(E^2 - \zeta^2)$ may be simplified by means of the continuity equation (10) to get $2 \left(\frac{\partial v}{\partial x} \frac{\partial u}{\partial y} - \frac{\partial u}{\partial x} \frac{\partial v}{\partial y} \right)$. Then

$$E^2 - \zeta^2 = -2\nabla^2\phi + 2f\zeta.$$

Therefore, an equation for the enstrophy is obtained:

$$\zeta^2 = 2\nabla^2\phi - 2f\zeta + E^2. \quad (12)$$

Now taking the derivative of (12), it can be seen that

$$\begin{aligned} \frac{\partial\zeta^2}{\partial t} &= 2\nabla^2\frac{\partial\phi}{\partial t} - 2f\frac{\partial\zeta}{\partial t} + \frac{\partial E^2}{\partial t} \\ &= -2fV_g \cdot \nabla \left(\frac{1}{f}\nabla^2\phi \right) + 2fV \cdot \nabla\zeta + \frac{\partial E^2}{\partial t}. \end{aligned}$$

Recall that by our assumptions,

$$\frac{\partial\zeta^2}{\partial t} = -V \cdot \nabla\zeta^2. \quad (13)$$

Thus by (13) we may write,

$$\begin{aligned}
-V \cdot \nabla \zeta^2 &= -2fV_g \cdot \nabla \zeta_g + 2fV \cdot \nabla \zeta + \frac{\partial E^2}{\partial t} \\
&= 2fV_{ag} \cdot \nabla (\zeta_g + \zeta) + \frac{\partial E^2}{\partial t} \\
&= 4fV_{ag} \cdot \nabla \zeta_g + 2fV_{ag} \cdot \nabla \zeta_{ag} + \frac{\partial E^2}{\partial t}, \quad (14)
\end{aligned}$$

where the relative vorticity ζ has been partitioned into its geostrophic and ageostrophic components. Hence, the enstrophy advection may be explained by the advection of geostrophic vorticity by the geostrophic wind – vorticity advection + the time tendency of squared total deformation. Moreover, it may be thought of as an advection by the ageostrophic wind also. A thorough investigation of how the terms interact to produce enstrophy will not be given here, but in later work by the authors.

7 Data

The data set used in this study was the National Center for Environmental Prediction (NCEP) and National Center for Atmospheric Research (NCAR) gridded re-analysis data [9]. These data were provided on 2.5° by 2.5° latitude-longitude grids available on 17 mandatory levels from 1000 mb to 10 mb at 6-h intervals daily at (<http://ersl.noaa.gov/psd/data/reanalysis/>). In this study, the u and v wind components were used in order to calculate the enstrophy advection.

8 Analysis

The blocking criterion given in [6] was used to determine the onset and decay times for the Northern Hemisphere blocking events shown in table 1, with the blocking intensity (BI) definition given in [11].

Date	BI	LON
January 6-12, 2012	3.69	60 E
January 9-16, 2012	3.55	20 W
January 12-27, 2012	5.01	130 W
January 17-29, 2012	3.61	60 E

Table 1: January 2012 blocking events. Block intensity and longitude at block onset.

In this short note only the contours of enstrophy advection for the block from Jan. 12-27, 2012 are provided. The analyses of the other blocks listed in table 1 are analogous to the Jan. 12-27 block and will be presented in further studies. Now, the

instability predicted by the IRE at block onset [7, 8] can be seen as contours of positive enstrophy advection over the region of the block in figures 1 and 2. The instability can be seen as solid contours of enstrophy advection over the blocking region, while stability can be seen as dashed contours.

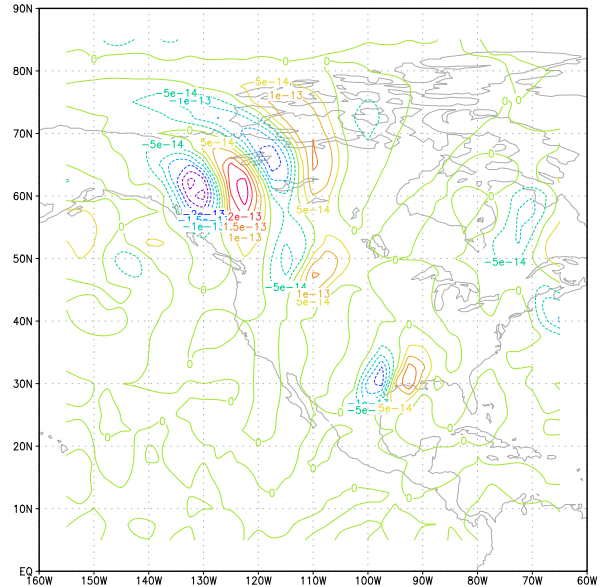


Figure 1: Jan. 11th contours of enstrophy advection. Block onset instability is shown. Solid contours are positive enstrophy advection, dashed contours are negative enstrophy advection.

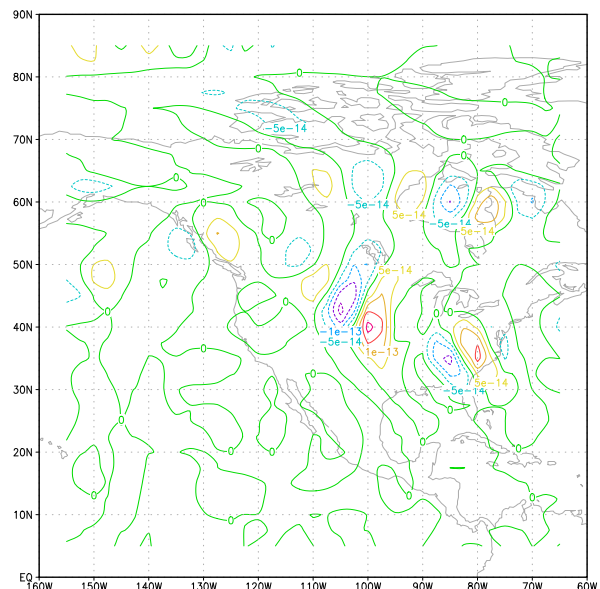


Figure 2: Jan. 12th contours of enstrophy advection. Block onset instability is shown.

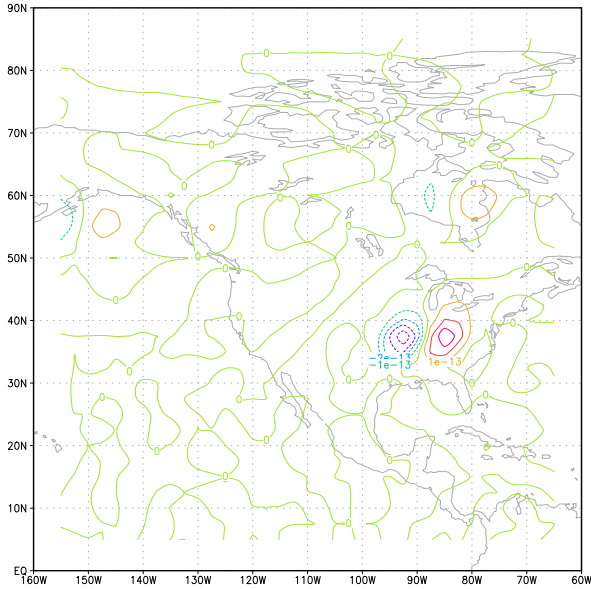


Figure 3: Jan. 13th contours of enstrophy advection. The block is beginning to stabilize.

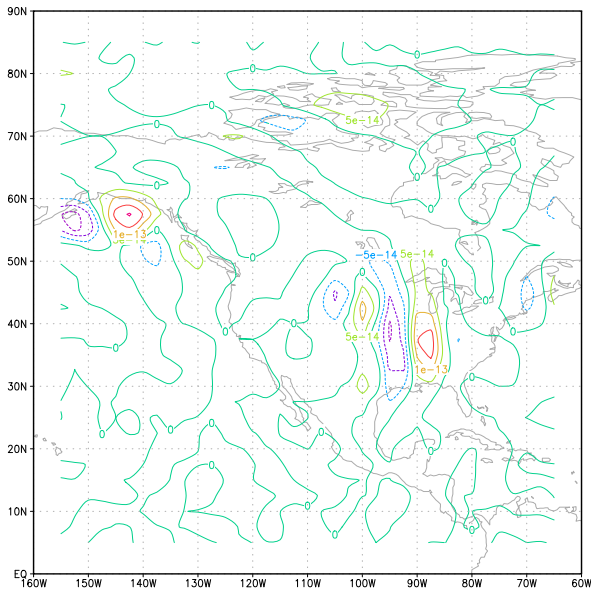


Figure 4: Jan. 27th contours of enstrophy advection. Block decay instability is shown.

By Jan. 13 (see figure 3) the instability from block onset is dying out and the block is stabilizing. Figure 4 shows a resurgence in instability at block decay, as predicted in [7, 8]. In section (4) it was shown that there should be a local maximum in instability between areas of negative enstrophy advection and positive enstrophy advection. Such areas can be seen in figures 1,2, and 4, indicating instability as was expected from the IRE [7].

9 Discussion

In [5] blocking was defined as a quasi-stationary state with a quasi-barotropic structure. In this short note, a barotropic structure has been employed as a model of the atmosphere to derive a new measure of stability/instability to identify blocking onset and decay: the enstrophy advection. Plots of enstrophy advection were provided for the Jan. 12-27, 2012 Northern Hemisphere blocking event. As can be seen in the plots, the enstrophy advection demarcates the instability and stability inherent in a blocking event as predicted by the IRE. Thus, the enstrophy advection was found to be a useful diagnostic. In addition, an equation relating enstrophy advection to ageostrophic vorticity advection and deformation tendency was derived.

References

- [1] H. Athar, and A.R. Lupo, 2010: Scale and stability analysis of blocking events from 2002-2004: A case study of an unusually persistent blocking event leading to a heat wave in the Gulf of Alaska during August 2004. *Adv. Met.*, **2010**, 15 pp, Article ID 610263, doi:10.1155/2010/610263.
- [2] F.J. Beron-Vera, M.J. Olascoaga, M.G. Brown, H. Kocak, and I.I. Rypina, 2010: Invariant-tori-like Lagrangian coherent structures in geophysical flows. *Chaos*, **20**, doi:10.1063/1.3271342.
- [3] S. Chen, R.E. Ecke, G.L. Eyink, X. Wang, and Z. Xiao, 2003: Physical mechanism of the two-dimensional enstrophy cascade. *Phys. Rev. Lett.*, **91**, doi:10.1103/PhysRevLett.91.214501.
- [4] R.A. Cohen, and D.M. Schultz, 2005: Contraction rate and its relationship to frontogenesis, the lyapunov exponent, fluid trapping, and airstream boundaries. *Mon. Wea. Rev.*, **133**, 1353-1369.
- [5] V.P. Dymnikov, Y.V. Kazantsev, and V.V. Kharin, 1992: Information entropy and local Lyapunov exponents of barotropic atmospheric circulation. *Izv. Atmos. Oceanic Phys.*, **28**, 425-432.
- [6] A.R. Lupo, and P.J. Smith, 1995: Climatological features of blocking anticyclones in the Northern Hemisphere. *Tellus*, **47A**, 439-456.

- [7] A.R. Lupo, I.I. Mokhov, S. Dostoglou, A.R. Kunz, and J.P. Burkhardt, 2007: The impact of the planetary scale on the decay of blocking and the use of phase diagrams and enstrophy as a diagnostic. *Izv. Atmos. Oceanic Phys.*, **42**, 45-51.
- [8] A.R. Lupo, I.I. Mokhov, M.G. Akperov, A.V. Cherkulsky, and H. Athar, 2012: A dynamic analysis of the role of the planetary and synoptic scale in the summer of 2010 blocking episodes over the European part of Russia. *Adv. Meteor.*, **2012**, Article ID 584257, 11 pp, doi:10.1155/2012/584257.
- [9] E. Kalnay, M. Kanamitsu, R. Kistler et al, 1996: The NCEP/NCAR 40-year reanalysis project. *Bull. Amer. Meteor. Soc.*, **77**, 437-471.
- [10] W.H. Matthaeus, and D. Montgomery, 1980: Selective decay hypothesis at high mechanical and magnetic Reynolds numbers. *Ann. N.Y. Acad. Sci.*, **357**, 203-222.
- [11] J.M. Wiedenmann, A.R. Lupo, I.I. Mokhov, and E. Tikhonova, 2002: The climatology of blocking anticyclones for the Northern and Southern Hemisphere: Block Intensity as a diagnostic. *J. Climate*, **15**, 3459-3473.
- [12] J. Weiss, 1991: The dynamics of enstrophy transfer in two-dimensional hydrodynamics. *Physica D*, **48**, 273-294.